Direct Evidence for the Protonation of Aspartate-75, Proposed To Be at a Quinol Binding Site, upon Reduction of Cytochrome bo_3 from *Escherichia coli*†

Petra Hellwig, Blanca Barquera, and Robert B. Gennis*

Department of Biochemistry, University of Illinois, 600 South Mathews Avenue, Urbana, Illinois 61801-3364

Received September 13, 2000; Revised Manuscript Received November 3, 2000

ABSTRACT: Aspartate-75 (D75) was recently suggested to participate in a ubiquinone-binding site in subunit I of cytochrome bo_3 from *Escherichia coli* on the basis of a structural model [Abramson, J., Riistama, S., Larsson, G., Jasaitis, A., Svensson-Ek, M., Laakkonen, L., Puustinen, A., Iwata, S., and Wikström, M. (2000) *Nat. Struct. Biol. 7* (10), 910−917]. We studied the protonation state of D75 for the reduced and oxidized forms of the enzyme, using a combined site-directed mutagenesis, electrochemical, and FTIR spectroscopic approach. The D75H mutant is catalytically inactive, whereas the more conservative D75E substitution has quinol oxidase activity equal to that of the wild-type enzyme. Electrochemically induced FTIR difference spectra of the inactive D75H mutant enzyme show a clear decrease in the spectroscopic region characteristic of protonated aspartates and glutamates. Strong variations in the amide I region of the FTIR difference spectrum, however, reflect a more general perturbation due to this mutation of both the protein and the bound quinone. Electrochemically induced FTIR difference spectra on the highly conservative D75E mutant enzyme show a shift from 1734 to 1750 cm^{-1} in direct comparison to wild type. After H/D exchange, the mode at 1750 cm^{-1} shifts to 1735 cm^{-1}. These modes, concomitant with the reduced state of the enzyme, can be assigned to the ν(C═O) vibrational mode of protonated D75 and E75, respectively. In the spectroscopic region where signals for deprotonated acidic groups are expected, band shifts for the $\nu(COO^-)^{s/as}$ modes from 1563 to 1554−1539 cm^{-1} and from 1315 to 1336 cm^{-1}, respectively, are found for the oxidized enzyme. These signals indicate that D75 (or E75 in the mutant) is deprotonated in the oxidized form of cytochrome bo_3 and is protonated upon full reduction of the enzyme. It is suggested that upon reduction of the bound ubiquinone at the high affinity site, D75 takes up a proton, possibly sharing it with ubiquinol.

Cytochrome bo_3 is a terminal oxidase in the aerobic respiratory chain of *Escherichia coli*. It catalyzes the two-electron oxidation of ubiquinol-8 and the four-electron reduction of dioxygen, and these reactions are coupled to the translocation of protons across the cytoplasmic membrane by a pumping mechanism (*1*−*3*). Most respiratory oxidases belong to the heme-copper oxidase superfamily, which includes the cytochrome *c* oxidases and the quinol oxidases. Despite differences in electron donating substrates (cytochrome *c*, ubiquinol), constituent heme species, and the presence or absence of a Cu_A center, the cytochrome *c* oxidases and the quinol oxidases appear to have the same mechanisms for reducing oxygen and for proton pumping.

The presence of two ubiquinol-8 binding sites with distinct functional roles has been proposed for cytochrome bo_3 from *E. coli* (*3*). In one possible mechanism, ubiquinone bound at a high affinity site, acting as a cofactor, mediates electron transfer from the ubiquinol substrate, which binds to a low affinity binding site, to the low-spin heme *b* (*3*−*6*). Reduced heme *b* then provides electrons to the heme-copper binuclear, formed by heme o_3 and Cu_B, where oxygen binds and is reduced to water.

The locations of the two proposed quinone binding sites within cytochrome bo_3 are not clear, and, indeed, direct unambiguous evidence that there are two different sites is lacking. There are considerable experimental indications from site-directed mutagenesis, photoaffinity labeling, and inhibitor-resistant mutants, that suggest that the low affinity site that binds to the substrate ubiquinol is located at least in part within subunit II of the enzyme (*6*−*8*). Recently, a chimeric construct was investigated, in which subunit II from a cytochrome *c* oxidase was exchanged with subunit II of cytochrome bo_3 oxidase from *E. coli* (*9*). This construct still exhibits ubiquinol oxidase activity, and this fact would appear to exclude many regions of subunit II from being involved in ubiquinol binding.

In addition to the deduced low affinity quinol binding site, cytochrome bo_3 from *E. coli* contains a tightly bound quinone, thought to be located at a different location within the enzyme. This tightly bound quinone can be isolated with the purified enzyme and, significantly, forms a stabilized ubisemiquinone radical that has been implicated as an intermediate during enzyme turnover (*10*−*13*). The semiquinone radical has been examined in detail by EPR and ENDOR spectroscopies, which indicate hydrogen bonding

† Financial support is gratefully acknowledged from DFG He-3150/1-1 for P.H. and a grant from the Department of Energy (DE-FG-02ER8713716) to R.B.G.

* To whom correspondence should be addressed: Department of Biochemistry, University of Illinois, 600 South Mathews Avenue, Urbana, IL 61801 USA; Telephone: 217-333-9075; FAX: 217-244-3186: E-mail: r-gennis@uiuc.edu.

10.1021/bi002154x CCC: $20.00
Published on Web 01/03/2001

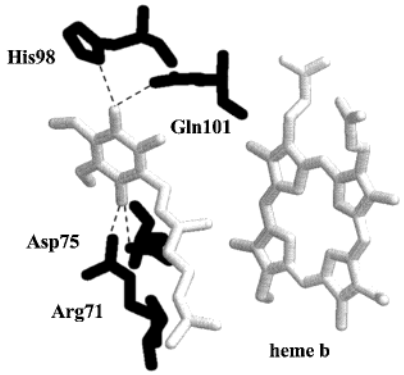

FIGURE 1: Position of D75 in relation to the modeled quinone in the structure of cytochrome bo_3 from *E. coli* as proposed by ref *16*.

to amino acid residues (*11*, *14*, *15*). Recently, the crystal structure of cytochrome bo_3 from *E. coli* was solved at about 3.5-Å resolution. In the model of the enzyme, although quinone cannot be resolved, amino acids presenting a feature able to bind ubiquinone were recognized (*16*), and a quinone binding site within subunit I was postulated based on the X-ray data. In the model, Q101 and H98 were proposed to interact with ubiquinone C4═O, whereas D75 and R71 were proposed as hydrogen bond partners to C1═O of the bound ubiquinone. This binding site is located in subunit I close to heme *b* and is shown in Figure 1. Site-directed mutants provide support for this model, insofar as several mutants result in strongly reduced quinol oxidase activity and increased K_m values for quinol oxidation (*16*). The purpose of the current work is to examine more closely mutational substitutions of D75 and to apply Fourier transform infrared (FTIR)[1] difference spectroscopy to probe possible changes in the state of ionization of this residue as well as perturbations to the bound quinone.

FTIR spectroscopy is a sensitive method to study the contributions of protonated aspartates and glutamates as exemplified by studies on the bacterial reaction center (*17*), rhodopsin (*18*), or cytochrome *c* oxidase (*19*, *20*). Previous recent studies examined the bound ubiquinone in cytochrome bo_3 from *E. coli* by FTIR spectroscopy and ^{13}C labeling (*21*) and identified vibrational modes of the bound ubiquinone. In the present work, electrochemical, FTIR spectroscopic, and site-directed mutagenesis methods are combined to test the proposal that D75 is at or near a quinone binding site. Creating a conservative mutation D75E and a strongly perturbing variation, D75H, the contributions of D75 and the protonation state of this residue in both the reduced and the oxidized forms of the enzyme were identified.

MATERIALS AND METHODS

Sample Preparation. For site-directed mutagenesis, an XmaI−HindIII fragment of the pJRHisA plasmid was cloned into pUC19 vector, and mutagenesis was performed according to the "Quick change" protocol of Stratagene. Mutant DNA was cloned back into pJRhisA (*22*) and transformed into GL101 (*23*). The mutations were confirmed by DNA sequencing (University of Illinois Biotechnology Center). The expression level of the D75E mutant enzyme was comparable to that of wild-type oxidase and of the D75H mutant was about 30%.

Cytochrome bo_3 enzyme from *E. coli* containing one equivalent of bound UQ_8 was purified in *n*-dodecyl-β-D-maltoside (DM) according to the method described by ref *22*. The oxidase activity assay of the purified protein was performed as previously described in ref *7* in Tris buffer, pH 7.4, and 0.1% DM and at 37 °C. For electrochemical experiments, the protein samples containing 100 mM phosphate buffer (pH 7), 100 mM KCl, and 0.1% DM were concentrated to approximately 0.4 mM using Microcon ultrafiltration cells (Millipore). H_2O was exchanged against D_2O by repeated concentration and dilution of the sample in the D_2O buffer. H/D exchange of amide I protons was found to be better than 70% as judged from the shift of the amide II mode at 1550 cm^{-1} in the FTIR absorbance spectra (data not shown).

Electrochemistry. The ultrathin layer spectroelectrochemical cell for the UV/VIS and IR detection and the potentiostat (Universitäts-Werkstatt, Freiburg) was a generous gift from Professor W. Mäntele (University of Frankfurt) and was used as previously described (*24*). Sufficient transmission in the range from 1800 to 1000 cm^{-1} was achieved with the path length of 6−8 μm. The gold grid working electrode was chemically modified by using a 2 mM cysteamine solution as described elsewhere (*20*). To accelerate the redox reaction, 16 different mediators were added including those listed by ref *20* except for *n*-methylphenazoniummethosulfate and *n*-ethylphenazoniumsulfate. The final concentration of each mediator was adjusted to 45 μM. At this concentration and at an optical path length below 10 μm, control experiments with protein-free samples revealed no contributions from the mediators in the VIS and IR spectral range, except for the P−O stretching modes of the phosphate buffer between 1200 and 1000 cm^{-1}. Potentials quoted with the data refer to the Ag/AgCl/3M KCl reference electrode (i.e., +208 mV for SHE′ at pH 7).

FTIR Difference Spectroscopy. FTIR difference spectra as a function of the applied potential were obtained in the 2500−1000 cm^{-1} range using a Biorad-575C instrument. In all experiments, the protein solution was first equilibrated at the initial potential of the electrode, and single beam spectra in the IR range were recorded. Then, a potential step toward the final potential was applied, and the single beam spectrum of this state was again recorded after equilibration. Subsequently, difference spectra, as presented in this work, were calculated from the two single-beam spectra with the initial single-beam spectrum taken as the reference. No smoothing or deconvolution procedures were applied. The equilibration at the applied potential generally took less than 4−5 min in the potential range from −0.5 to 0.5 V for the protein concentration, type, and concentration of the mediators, and electrode modification described above. Equilibration times have been determined with UV/Vis difference spectra on the same sample (data not shown), and the full reaction in the FTIR was monitored by double difference spectra until no changes were detected. Typically, 320 interferograms at 4 cm^{-1} resolution were co-added for each single-beam IR spectrum and Fourier transformed using triangular apodization. A total of 5 to 10 difference spectra were usually averaged. The noise level in the difference spectra was estimated to be around $30-50 \times 10^{-6}$ absor-

[1] Abbreviations: FTIR: Fourier transform infrared; SHE′, standard hydrogen electrode; UQ, ubiquinone; DM, *n*-dodecyl-β-D-maltoside.

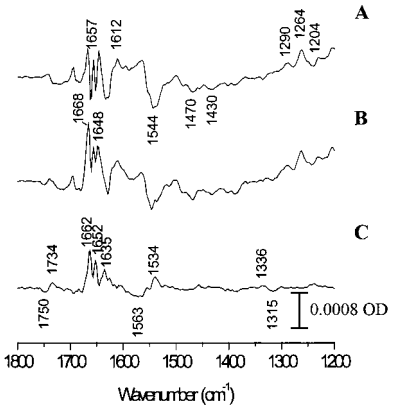

FIGURE 2: Oxidized-minus-reduced FTIR difference spectrum of wild-type (A) D75E mutant enzyme (B) and double difference spectra obtained by subtracting the electrochemically induced FTIR difference spectra of wild-type from D75E (C) in the spectral range from 1800 to 1200 cm^{-1} and a potential step from −0.5 to 0.5 V.

bance units in the spectral range under consideration, except for the region of the strongly absorbing water bending and protein amide I modes at ca. 1650 cm^{-1} where the noise was slightly higher.

RESULTS

Oxidase Activity and UV/Vis Spectra of the Mutants. Quinol oxidase activity measured polarographically at an oxygen electrode yielded wild-type activity for the D75E mutant cytochrome bo_3 and a complete loss of activity for the D75H mutant enzyme. Wild-type and the D75E mutant enzyme have the same K_m value for ubiquinol-1 oxidation. UV/Vis spectra of purified protein indicate no perturbation due to the D75E mutation and a small shift of the Soret band from 409 to 406 nm, for the oxidized form of the D75H mutant.

Electrochemically Induced FTIR Difference Spectra of D75E. Figure 2 shows the oxidized-minus-reduced FTIR difference spectrum of the wild-type and D75E mutant enzymes for a potential step from −0.5 to 0.5 V. Figure 2, panel C, shows a double difference spectrum obtained by subtracting the electrochemically induced FTIR difference spectra of wild type from that of D75E. In the electrochemically induced FTIR difference spectra of the D75E mutant enzyme and the corresponding double difference spectrum, a shift of a negative mode from 1734 to 1750 cm^{-1} can be seen (Figure 2). In the amide I range, there is an increase of the modes at 1662, 1657, and at 1635 cm^{-1}, and in the amide II range, there is a shift from 1563 cm^{-1} to a double peak at 1554/1539 cm^{-1}. There is also a shift of a band from 1315 to 1336 cm^{-1} observed in the double difference spectrum in Figure 2, panel C.

In the electrochemically induced FTIR difference spectra, contributions concomitant with electron transfer to/from the cofactors (hemes *b* and o_3, Cu_B and UQ) can be expected from the reorganization of hemes *b* and o_3, the tightly bound ubiquinone, secondary structure elements, and from individual amino acids. Furthermore, redox coupled proton translocations, either from net proton uptake/release or internal shifts within the protein, will contribute to the FTIR-detected changes.

As discussed below, there is a solid experimental basis to make assignments of specific FTIR bands and interpret these in terms of redox-induced changes in D75. Previous studies include those on isolated amino acids in solution, as well as FTIR difference spectroscopy with cytochrome bo_3 and other proteins by several groups, including assignments made by site-directed mutagenesis and by isotope labeling (see below).

Contributions in the Amide I Range (1690−1620 cm^{-1}). In the amide I range, difference signals at 1670, 1657, 1648, and 1630 cm^{-1} indicate absorbance changes of C═O modes caused by small, redox-induced alterations in the polypeptide backbone, as well as possible contributions from C═O modes of individual amino acid side chains (Asn and Gln). Besides, contributions of the ν(C═O) and ν(C═C) vibrational mode of the tightly bound quinone are present at 1657 and 1612 cm^{-1}, respectively. The assignments of the ubiquinone vibrational modes in cytochrome bo_3 from *E. coli* have recently been obtained on the basis of ^{13}C labeled isotopomers (*21*). Several shifts in the amide I region occur in the electrochemically induced FTIR difference spectra of the D75E mutant enzyme. The increase of the mode at 1668 cm^{-1}, may represent an upshift of the ν(C═O) mode of the bound quinone resulting from weaker hydrogen bonding, which is also evident with the upshift of the E75 ν(C═O) mode from 1738 to 1750 cm^{-1} (see below). Additionally, variations of the neighboring R71, which has also been proposed to be engaged in ubiquinone binding (*16*), can be tentatively assigned to modes at 1662 and 1635 cm^{-1}. Contributions of isolated arginines in solution have been observed: the $\nu(CN_3H_5^+)^{as}$ vibrational mode at 1672 cm^{-1} and $\nu(CN_3H_5^+)^{s}$ vibrational mode at 1633−1636 cm^{-1} (*25*). Arginine modes have also been observed between 1688 and 1695 cm^{-1} in halorhodopsin (*26*). The assignment of the 1662 and 1635 cm^{-1} bands to arginine (R71, specifically), however, is just speculative and must be confirmed by further mutagenesis and isotope labeling experiments. Variations at the polypeptide backbone cannot be excluded to be involved in the shifts discussed here, but this does not appear likely, based on the highly conservative character of the D75E variant.

Contributions in the Amide II Range (1570−1520 cm^{-1}). In the amide II range, coupled CN stretching and NH bending modes are expected. Vibrational modes from aromatic amino acids and C═C modes from the heme porphyrin ring are conceivable. Antisymmetric COO^- modes from deprotonated heme propionates and Asp or Glu side chains, caused by protonation/deprotonation of COOH groups, may also contribute here (*25*, *27*, *28*). On this basis, the shift at 1563 to 1554/1534 cm^{-1} due to the D75E mutation is tentatively attributed to the $\nu(COO^-)^{as}$ vibrational mode, reflecting the deprotonated forms of D75 and E75, respectively. Probably, additional variations are involved in the double peak observed at 1554−1534 cm^{-1}, such as a perturbation of the hemes. The corresponding $\nu(COO^-)^{s}$ vibrational mode of deprotonated aspartic and glutamic acids is expected between 1450 and 1300 cm^{-1} and can be seen at 1315 and 1336 cm^{-1}. Whereas the ν(C═O) mode of the fully protonated form, as well as the $\nu(COO^-)^{s}$ vibrational mode, shift to higher wavenumbers upon mutation from D75 to E75, a downshift of the $\nu(COO^-)^{as}$ vibrational mode is observed. This is in line with weaker hydrogen bonding for both the protonated and the deprotonated states of E75 in comparison to D75.

Contributions in the Spectral Range from 1500 to 1000 cm^{-1}. In addition to the C═O and the C═C modes of the

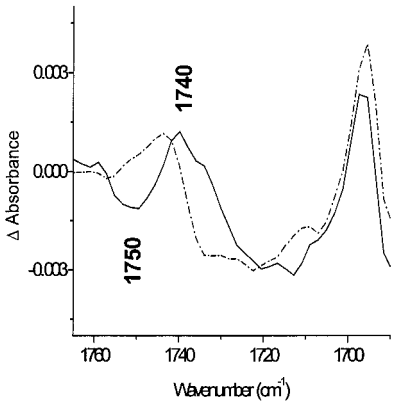

FIGURE 3: Enlarged view of the oxidized-minus-reduced FTIR difference spectrum of wild type (dotted line) and D75E (full line) in the spectral range from 1765 −1690 cm^{-1} and a potential step from −0.5 to 0.5 V.

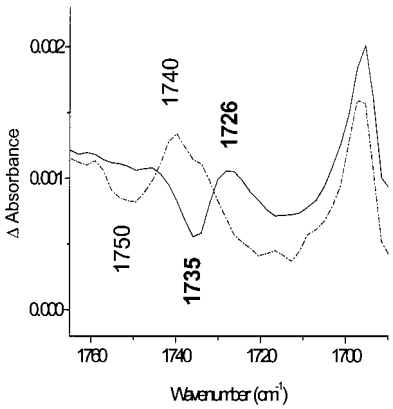

FIGURE 4: Oxidized-minus-reduced FTIR difference spectrum of D75E mutant enzyme equilibrated in H_2O (dotted line) and D_2O (full line) in the spectral range from 1765 to 1690 cm^{-1} and a potential step from −0.5 to 0.5 V.

fully oxidized ubiquinone, mentioned above, modes involving coordinates of the methoxy group are involved in the signals at 1290, 1264, and 1204 cm^{-1} (*21*). The ring modes of the fully reduced and protonated form of ubiquinol contribute to the signals at 1486, 1470, 1430, and 1386 cm^{-1}. No significant change in this portion of the difference spectrum is seen upon mutation of D75 to either D75E or D75H. Interestingly, the bound quinone is still present in the D75H mutant, although this enzyme is catalytically inactive. Below 1200 cm^{-1}, the strong differential modes of the ν(P═O) phosphate buffer are present (data not shown), reflecting the proton uptake/release of the buffer upon electron transfer to/from the protein and the mediators (*20*, *29*).

Contributions of Protonated Aspartatic and Glutamic Acids (1760−1710 cm⁻¹). Figure 3 shows the enlarged view of the oxidized-minus-reduced FTIR difference spectra of wild type (dotted line) and D75E (solid line) mutant enzyme from 1765 to 1690 cm^{-1} for a potential step from −0.5 to 0.5 V.

In the spectroscopic range above 1710 cm^{-1}, the ν(C═O) vibrational modes from protonated Asp and Glu are expected, based on the reported IR spectra of isolated aspartic and glutamic acid in solution (*25*), as well as from difference FTIR spectroscopy on proteins and corresponding assignments by site-directed mutants (see for example refs *17* and *18*). On this basis, the shift of a mode from 1738 to 1750 cm^{-1} can be assigned to the ν(C═O) mode of D75, protonated in the reduced form. The corresponding IR signal concomitant with the introduced E75 contributes at a higher wavenumber, apparently reflecting a small variation in the environment of the carbonyl group, such as weaker hydrogen bonding resulting from a change in location of the COOH due to the longer side chain. The spectra of protonated aspartic and glutamic acids in solution differ by only 4 cm^{-1} (*25*), but the protein environment is the more dominating factor here, leading to a shift of 12 cm^{-1}. Alternatively, differential infrared signals comparing D75 and the D75E mutant could arise if E75 were fully protonated in both oxidized and reduced forms and experiencing an environmental change. However, since the D75E mutant remains fully active, it seems unlikely that it would behave so differently from the wild type D75, which clearly is deprotonated in the oxidized state.

In previous work with cytochrome bo_3 from *E. coli*, the redox difference signals at 1744/1722 cm^{-1} were assigned to the COOH mode of E286 (*30*−*32*). The spectra induced by photoreduction (*31*, *32*) lead to spectra comparable to those induced electrochemically, shown here. Yamazaki et al. (*32*) show that for the E286D mutant, there is a shift of the 1744/1722 cm^{-1} modes. Lübben et al. (*32*), however, describes a simple intensity decrease of modes at 1745/1735 cm^{-1} and not a frequency shift, upon mutation of E286 to D. The reasons for the discrepancy of about 13 cm^{-1} between the wild type spectra and for the different reported effects of the E286D mutation are unclear. Differences in sample preparation are possible, yielding enzymes with different contents of bound quinone. It is noted that in a study examining the electrochemically induced FTIR difference spectrum of the cytochrome *c* oxidase from *Paracoccus denitrificans*, the analogous signals at 1746/1734 cm^{-1} were attributed to a shift of the COOH modes of Glu278, the amino acid corresponding to E286 in the numbering of *P. denitrificans* (*20*).

Figure 4 shows the enlarged view of the oxidized-minus-reduced FTIR difference spectra from 1765 to 1690 cm^{-1} of the D75E mutant enzyme equilibrated in H_2O (dotted line) and D_2O buffer (solid line) for a potential step from −0.5 to 0.5 V. A shift from 1750 to 1735 cm^{-1} and from 1740 to 1726 cm^{-1} is observed upon H/D exchange. The broad negative signal at approximately 1720 cm^{-1} is overlapped by the mode at 1676 cm^{-1}. For protonated side chains of Asp and Glu residues in model compounds, a shift of about 10 cm^{-1} is observed upon H/D exchange (*25*) and has been observed to be 4−12 cm^{-1} for proteins (*17*−*19*). The shifts observed here thus strengthen the assignment of the D75/E75 ν(C═O) COOH modes.

Electrochemically Induced FTIR Difference Spectra of D75H. Figure 5 shows the oxidized-minus-reduced FTIR difference spectrum of (A) the wild-type cytochrome bo_3, and (B) the D75H mutant enzyme, for a potential step from −0.5 to 0.5 V. Figure 5, panel C, shows a double difference spectrum obtained by subtracting the electrochemically induced FTIR difference spectra of the wild type from that of D75H. Because of instability of the mutant enzyme during the redox potentiometry, only a few redox cycles were performed, leading to a reduced signal-to-noise ratio. In the electrochemically induced FTIR difference spectrum of the

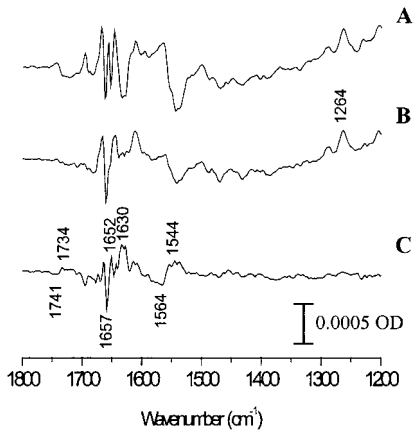

FIGURE 5: Oxidized-minus-reduced FTIR difference spectrum of wild type (A), D75H mutant enzyme (B), and double difference spectra obtained by subtracting the electrochemically induced FTIR difference spectra of wild type from D75H (C), for a in the spectral range from 1800 to 1200 cm^{-1} and a potential step from −0.5 to 0.5 V.

D75H mutant enzyme and in the corresponding double difference spectrum (wild type-minus-D75H) strong perturbations can be seen. Modes between 1760 and 1710 cm^{-1} are strongly decreased in intensity. In the amide I range, a shift of the mode at 1657 to 1652 cm^{-1} is observed (Figures 5, panels B and C). The mode at 1630 cm^{-1} is strongly decreased in intensity, and signals at 1686 and 1668 cm^{-1} are perturbed. In the amide II region, there is a decreased intensity of broad bands at 1564 and 1544 cm^{-1}.

The band that shifts from 1657 to 1652 cm^{-1} is tentatively attributed to the ν(C═O) vibrational mode of ubiquinone. Ubiquinone is still present in the D75H protein preparation, as indicated by the most prominent mode at 1264 cm^{-1}. Possibly in the D75H mutant, the quinone is bound differently or is weakly bound to the high affinity site, leading to the observed shift of the ν(C═O) mode from 1657 to 1652 cm^{-1}. A perturbation of the polypeptide backbone could also cause this shift and is likely the cause of the variations at 1686 and 1630 cm^{-1}. In general, the electrochemically induced FTIR difference spectra reflect a general perturbation of the protein due to the D75H mutation, making detailed analysis unwarranted since any effects may be not specifically associated with the immediate location of the mutation within the protein. The nearly complete loss of the modes in the spectroscopic range of protonated Asp and Glu residues from 1760 to 1710 cm^{-1}, which includes the contribution of Glu 286, clearly reflects a major structural perturbation due to the D75H mutation. Note that the UV/Vis spectra show only a small shift of the Soret band of the oxidized form from 409 to 406 nm and is a much less sensitive indicator of protein perturbation than the FTIR difference spectra.

DISCUSSION AND CONCLUSIONS

Previous spectroscopic studies of the tightly bound quinone by EPR (*11*, *33*), FTIR (*21*), and ENDOR spectroscopy (*14*, *15*) as well as detailed inhibitor binding studies (*34*−*36*) provide important information about the structure and orientation of the bound quinone and quinone-analogue inhibitors. EPR spectroscopy studies have shown that the tightly bound quinone can be stabilized as a semiquinone anion radical in the protein (*10*, *11*). On the basis of a combined FTIR spectroscopy and ^{13}C labeling approach, it was demonstrated that the fully oxidized, bound quinone, as well as the reduced and protonated quinol, is hydrogen bonded to the protein matrix and that the hydrogen bonding is both weak and symmetrically oriented (*21*). FTIR as well as several inhibitor studies suggest that the 2-methoxy group of ubiquinone is sterically hindered, whereas the 3-methoxy group is free from steric constraints (*21*, *34*). Recent ENDOR work shows strong interaction with the C1−O (*14*). Hastings et al. (2000) suggest a symmetrical binding for both C1−O and C4−O groups of the semiquinone anion radical. A structural model, based on X-ray crystallography, suggests that the amino acid D75 is one of the hydrogen bonding partners at the quinol binding site (*16*).

In the current work, electrochemically induced FTIR difference spectra of the D75E mutant cytochrome bo_3 from *E. coli* show that D75 is protonated upon reduction of the protein and quinone. The D75N mutant enzyme was reported only to have 1% turnover (*16*), and the D75H mutant presented in the current work is totally inactive. The work presented here is, thus, consistent with the presence of D75 at the quinone binding site and suggests an important functional role for this residue. It is noteworthy that D75E is fully functional, though the hydrogen bond, as revealed by electrochemically induced FTIR difference spectra, is considerably weaker than that of wild type D75. Although the precise function of the quinone at the high affinity site is not yet fully clarified, it appears that D75 plays an important role in proton movements within the protein during catalytic turnover. An interaction with the semiquinone anion is conceivable and appears very likely.

The data show that mutations of D75 perturb the bound quinone and that D75 is protonated, possibly in direct response to reduction of the bound quinone. However, to prove that D75 is located at the site where the semiquinone radical is formed, further EPR and ENDOR experiments will be necessary. Such experiments are currently underway.

ACKNOWLEDGMENT

We are indebted to Professor Dr. Werner Mäntele (University of Frankfurt) for providing the electrochemical cell and potentiostat used here. We are grateful to Professor Dr. So Iwata (University of London) and colleagues for providing the coordinates of the cytochrome bo_3 structure prior to publication and to Dr. Anne Puustinen (University of Helsinki) for providing the Q101N and H98F mutant enzymes prior to publication.

REFERENCES

1. Calhoun, M. W., Thomas, J. W., and Gennis, R. B. (1994) *Trends Biol. Sci. 19*, 325−330.
2. Garcia-Horsman, J. A., Barquera, B., Rumbley, J., Ma, J., and Gennis, R. B. (1994) *J. Bacteriol. 176*, 5587−5600.
3. Mogi, T., Tsubaki, M., Hori, H., Miyoshi, H., Nakamura, H., and Anraku, Y. (1998) *J. Biochem. Mol. Biol. Biophys. 2*, 79−110.
4. Sato-Watanabe, M., Mogi, T., Ogura, T., Kitagawa, T., Miyoshi, H., Iwamura, H., and Anraku, Y. (1994) *J. Biol. Chem. 269*, 28908−28912.
5. Sato-Watanabe, M., Mogi, T., Miyoshi, H., and Anraku, Y. (1998) *Biochemistry 37*, 5355−5361.
6. Sato-Watanabe, M., Mogi, T., Sakamoto, K., Miyoshi, H., and Anraku, Y. (1998) *Biochemistry 37*, 12744−12752.

7. Ma, J., Puustinen, A., Wikström, M., and Gennis, R. B. (1998) *Biochemistry 37*, 11806−11811.
8. Tsatsos, P. H., Reynolds, K., Nickels, E. F., He, D.-Y., Yu, C.-A., and Gennis, R. B. (1998) *Biochemistry 37*, 9884−9888.
9. Sakamoto, K., Mogi, T., Noguchi, S., and Sone, N. (2000) *J. Biochem. 126*, 934−939.
10. Sato-Watanabe, M., Itoh, S., Mogi, T., Matsuura, K., Miyoshi, H., and Anraku, Y. (1995) *FEBS Lett. 374*, 265−269.
11. Ingledew, W. J., Ohnishi, T., and Salerno, J. C. (1995) *Eur. J. Biochem. 227*, 903−908.
12. Osborne, J. P., Musser, S. M., Schultz, B. E., Edmondson, D. E., Chan, S. I., and Gennis, R. B. (1998) in *Oxygen Homeostasis and Its Dynamics* (Ishimura, Y., Shimada, H., and Suematsu, M., Eds.) pp 33−39, Springer-Verlag, Tokyo.
13. Schultz, B. E., Edmondson, D. E., and Chan, S. I. (1998) *Biochemistry 37*, 4160−4168.
14. Veselov, A. V., Osborne, J. P., Gennis, R. B., and Scholes, C. P. (2000) *Biochemistry 39*, 3169−3175.
15. Hastings, S., Heathcote, P., Ingledew, W. J., and Rigby, S. E. J. (2000) *Eur. J. Biochem. 267*, 5638−5645.
16. Abramson, J., Riistama, S., Larsson, G., Jasaitis, A., Svensson-Ek, M., Laakkonen, L., Puustinen, A., Iwata, S., and Wikström, M. (2000) *Nature Struct. Biol. 7*, 910−917.
17. Hienerwadel, R., Grzybek, S., Fogel, C., Kreutz, W., Okamura, M. Y., Paddock, M. L., Breton, J., Nebedryk, E., and Mäntele, W. (1995) *Biochemistry 34*, 2832−2843.
18. Fahmy, K., Jager, F., Beck, M., Zvyaga, T. A., Sakmar, T. P., and Siebert, F. (1993) *Proc. Natl. Acad. Sci. U.S.A. 90*, 10206−10210.
19. Hellwig, P., Rost, B., Kaiser, U., Ostermeier, C., Michel, H., and Mäntele, W. (1996) *FEBS 385*, 53−57.
20. Hellwig, P., Behr, J., Ostermeier, C., Richter, O.-M. H., Pfitzner, U., Odenwald, A., Ludwig, B., Michel, H., and Mäntele, W. (1998) *Biochemistry 37*, 7390−7399.
21. Hellwig, P., Mogi, T., Tomson, F. L., Gennis, R. B., Iwata, J., Miyoshi, H., and Mäntele, W. (1999) *Biochemistry 38*, 14683−14689.
22. Rumbley, J. N., Nickels, E. F., and Gennis, R. B. (1997) *Biochim. Biophys. Acta 1340*, 131−142.
23. Lemieux, L. J., Calhoun, M. W., Thomas, J. W., Ingledew, W. J., and Gennis, R. B. (1992) *J. Biol. Chem. 267*, 2105−2113.
24. Moss, D., Nabedryk, E., Breton, J., and Mäntele, W. (1990) *Eur. J. Biochem. 187*, 565−572.
25. Venyaminov, S. Y., and Kalnin, N. N. (1990) in *Biopolymers*, pp 1243−1257, John Wiley & Sons, Inc.
26. Rudiger, M., Haupts, U., Gerwert, K., and Oesterhelt, D. (1995) *EMBO J. 14*, 1599−1606.
27. Fahmy, K., Weidlich, O., Engelhard, M., Sigrist, H., and Siebert, F. (1993) *Biochemistry 32*, 5862−5869.
28. Behr, J., Hellwig, P., Mäntele, W., and Michel, W. (1998) *Biochemistry 37*, 7400−7406.
29. Baymanm, F., Robertson, D. E., Dutton, P. L., and Mantele, W. (1999) *Biochemistry 38*, 13188−13199.
30. Puustinen, A., Bailey, J. A., Dyer, R. B., Mecklenburg, S. L., Wikström, M., and Woodruff, W. H. (1997) *Biochemistry 36*, 13195−13200.
31. Lübben, M., Prutsch, A., Mamat, B., and Gerwert, K. (1999) *Biochemistry 38*, 2048−2056.
32. Yamazaki, Y., Kandori, H., and Mogi, T. (1999) *J. Biochem. 126*, 194−199.
33. Mogi, T., Hirano, T., Nakamura, H., Anraku, Y., and Orii, Y. (1995) *FEBS Lett. 370*, 259−263.
34. Sakamoto, K., Miyoshi, H., Takegami, K., Mogi, T., Anraku, Y., and Iwamura, H. (1996) *J. Biol. Chem. 271*, 29897−29902.
35. Musser, S. M., Stowell, M. H. B., Lee, H. K., Rumbley, J. N., and Chan, S. I. (1997) *Biochemistry 36*, 894−902.
36. Sato-Watanabe, M., Mogi, T., Miyoshi, H., Iwamura, H., Matsushita, K., Adachi, O., and Anraku, Y. (1994) *J. Biol. Chem. 269*, 28899−28907.

BI002154X